Experimental Evaluation of Cyclic Behavior of Concrete Filled Steel Battened Columns

Mehrdad Zare Dastjerdian[1] and Majid Mohammadi[2*]

1. Ph.D. Candidate, Structural Engineering Research Center, International Institute of Earthquake Engineering and Seismology (IIEES), Tehran, Iran
2. Associate Professor, Structural Engineering Research Center, International Institute of Earthquake Engineering and Seismology (IIEES), Tehran, Iran,
*Corresponding Author; email: m.mohammadigh@iiees.ac.ir

ABSTRACT

Steel battened columns have been widely used in semi-rigid frames in last decades in some countries including Iran. In past earthquakes, severe failure under lateral actions was observed in residential and industrial buildings with such structural system. Many retrofitting or repairing methods have been proposed including adding some steel plates to the columns in order to change their section to a box. These methods are not only expensive and hard but also did not strengthen the columns at the connection with beams. Therefore, this paper has focused on a new innovative method; filling the battened columns with concrete, which has been previously applied for steel tubes. In this experimental and analytical program on seven specimens, axial load level and batten spacing intervals were considered as the key variables. The obtained results showed that the concrete filled battened columns can provide a stable cyclic response with enhanced lateral strength, higher dissipated energy and ductility, in comparison with the hollow one; the average improvement in the lateral strength and energy dissipation were recorded as about 30% and 300%, respectively, in comparison with the hollow ones. Furthermore, it is shown that capacity modification factor of a concrete-filled specimen is up to 47% higher than that of the similar hollow one. Regarding that filling with concrete raises both the ductility and strength. This method is highly recommended to strengthen fragile hollow battened columns.

1. Introduction

Built-up steel battened columns (SBC) are composed of two or more similar longitudinal chords connected by horizontal connectors along their height. In accordance with Iranian National building code part 10 [1] and international building codes such as AISC360-05 [2], this type of built-up columns are used as compression members to experience axial action without any lateral seismic loading. However, utilizing the SBCs has been previously a common construction practice in Iran, and hence, several failure modes have been observed during the recent earthquakes in Iran, as shown in Figure (1).

2. Typical Behavior of Regular Steel Battened Columns

Limited studies performed on the cyclic lateral behavior of SBCs showed that severe local buckling at the bottom is the dominant failure mode [3-4].

Hosseini Hashemi and Jafari [5] and Hosseini Hashemi and Poursamad Bonab [6-7] evaluated the cyclic lateral behavior of double I-section SBCs in the presence of axial constant force.
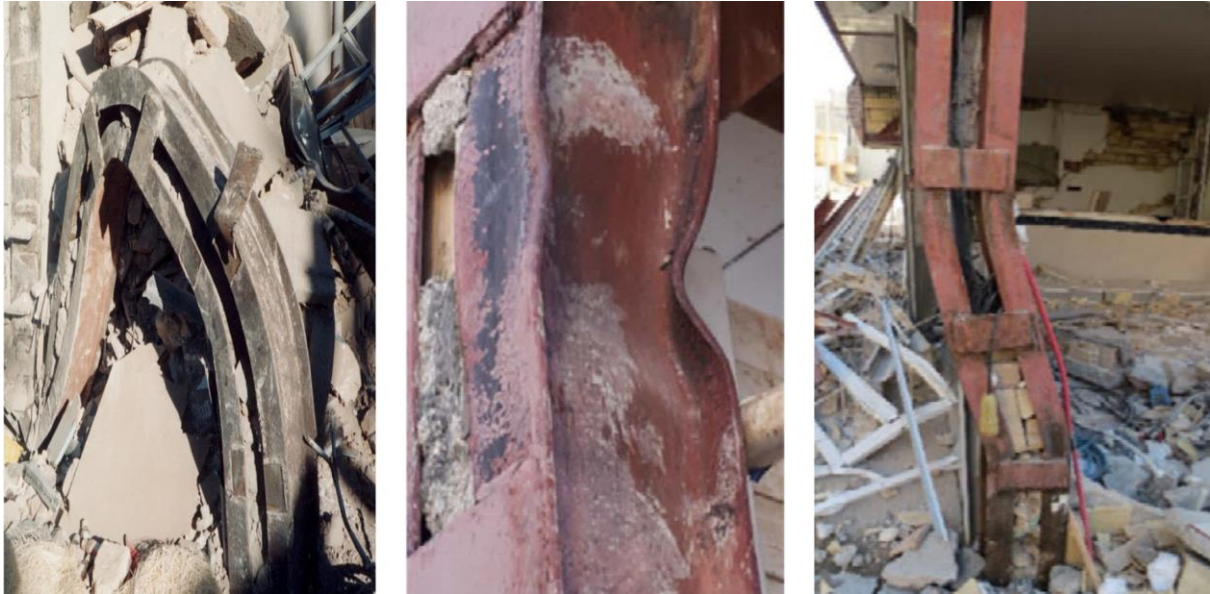
Figure 1. Failure of steel battened columns in Bam and Sarpol-e Zahab earthquakes [8-9].

The results have been affected mainly by axial force level in comparison with the battens spacing and profiles distance. Narrow hysteresis loops, severe local buckling and brittle performance at middle and high axial force level were observed. Hysteresis curves showed growth in the strength until webs local buckling started. After that, positive slope of loops was reduced till flatting and then descending curve occurred [5].

3. Cyclic Behavior of In-Filled Steel Chords

Concrete-filled steel columns have been a major subject of interest in order to enhance the strength and cyclic response of steel components having tube, box and pipe sections. According to results, the cyclic performance of concrete-filled steel tubes was mainly governed by cross-sectional and overall slenderness ratios [10-25]. In thin-walled, filled steel boxes, the interior diaphragms and partial filling also had a considerable effect on the cyclic response of filled columns [26-29].

Few research studies have been carried out on the behavior of concrete-filled battened columns (CFBC), mainly focused on the axial capacity of CFBCs and bonding effects: Hunaiti et al. [30] investigated the effect of bonding at the interface of concrete and steel on the axial strength of large scale samples with double channel sections.

Actual axial strength was much greater than the calculated strength, and the bonding had no major effect on the behavior of the specimen. Taylor et al. [31] performed an experimental investigation to identify the effect of bond strength on the load carrying and ductility capacity of filled double channel columns under the eccentric axial monotonic compression load. The results showed that the steel-concrete bonding has a negligible effect on the load-carrying capacity of CFBCs and indicated that ductility was decreased by increasing the eccentricity of the axial load.

Elzbieta et al. [32] and Zoltowski et al. [33-34] have performed a comprehensive experimental and analytical research on twenty full-scale double H-shaped concrete-filled columns under pure axial loading. According to the results, by decreasing the batten plate intervals, the axial capacity of specimens increased noticeably.

Mehrabani et al. [35] and Venugopal et al. [36] tested and simulated three steel battened columns and three encased ones under pure axial load. According to results, the compressive strength of concrete has a significant effect on the ultimate strength of composite columns with a low global slenderness ratio.

4. Test Specimens

In the present study, the experiments were

conducted on seven samples with cantilever configuration: six concrete-filled and one hollow steel battened column. All Specimens were fixed at the bottom and hinged on the top, representing half of a steel column condition. The specimens were installed on a 40 mm thick steel plate with six stiffener plates to simulate the fixed end condition at the bottom end. All specimens were built-up by two IPE100 sections with a distance of 120 mm and a height of 1200 mm. For the concrete-filled specimens, the gap between the battens covered by wooden sheets and filled with concrete (Figure 2).

The concrete core was cured at standard temperature and humidity for 28 days (Figure 3).

The studied specimens, listed in Table (1), were different in batten spacing and axial load levels, but similar in lateral loading protocol. A three-part-name was chosen for each specimen: the first character, "*H*" or "*F*", means being
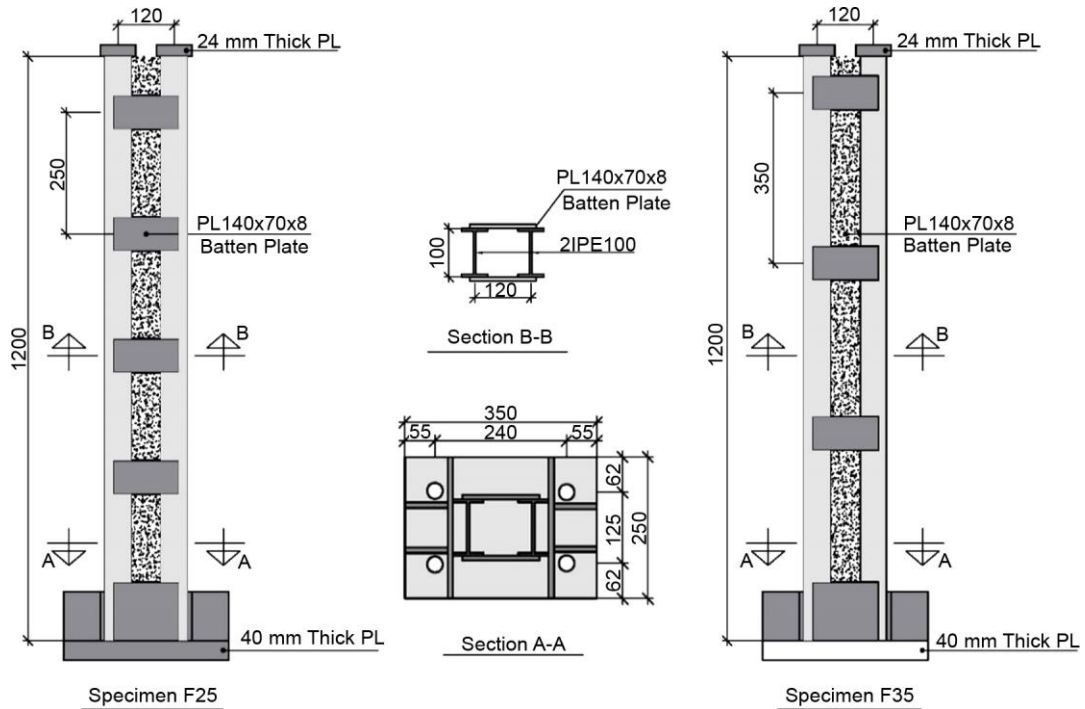

Figure 2. Detailing and dimensions of specimens (dimensions in mm).

(a) Steel member installation   (b) Formwork installation and filling with concrete   (c) Formwork removing

Figure 3. Construction process of concrete-filled specimens.

Table 1. Dimensions of the structural battened column specimens.

Dimension	Specification	Batten Spacing (mm)	Axial Load
H35P1	Hollow	350	$0.15P_y$
F35P1	Filled with Concrete	350	$0.15P_y$
F35P2	Filled with Concrete	350	$0.30P_y$
F35P3	Filled with Concrete	350	$0.40P_y$
F25P1	Filled with Concrete	250	$0.15P_y$
F25P2	Filled with Concrete	250	$0.30P_y$
F25P3	Filled with Concrete	250	$0.40P_y$

Table 2. Dimensions of the structural battened column specimens.

Component	Yield Stress (MPa)	Ultimate Stress (MPa)	Young Modulus (GPa)
Chord Flang	313.6	341.0	216.8
Chord Web	251.3	263.1	198.5

To determine the mechanical properties of concrete, some standard cubic samples were cured for 28 days and then tested under uniaxial compression. According to ACI318-11 [37], cubic compressive strength converted to standard cylindrical and averaged (Table 3).

Table 3. Mechanical properties of concrete.

Component	Cylindrical Compressive Stress (MPa)	Standard Deviation (MPa)
Concrete	48.45	4.24

hollow or filled with concrete, respectively. The second one is a number representing the distance between battens and the last part is for the value of the axial compression. "*P*1", "*P*2" and "*P*3" corresponds to 0.15 P_y, 0.30 P_y, and 0.40 P_y, respectively. P_y is the yielding strength of the hollow column sample, calculated according to AISC360-05 [2] as follows:

$$P_y = Fy\,A \qquad (1)$$

where A_g is the total cross-sectional area and P_y is the yield stress of the chord steel.

As shown in Table (1), all specimens except the H35P1 were filled with concrete.

5. Material Properties

Mechanical properties of steel sections were measured, based on the coupon tests, prepared from the section web and flange. The results are shown in Figure (4) and summarized in Table (2).
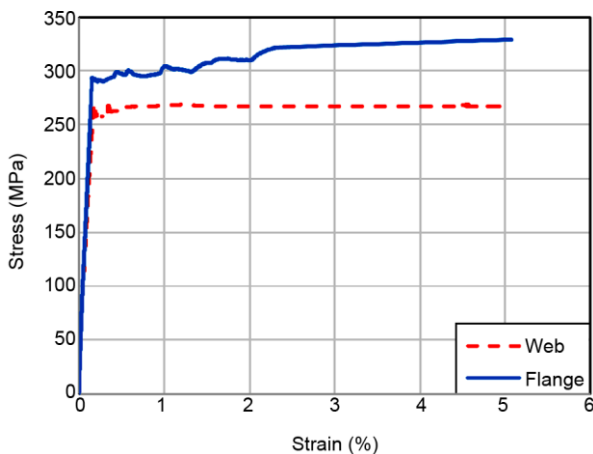

Figure 4. Uniaxial stress- strain curve of steel material.

6. Test Set-Up and Instrumentation

The vertical axial load and horizontal cyclic displacement were applied by 500 kN and 250 kN hydraulic actuators respectively, as shown in Figure (5a). High-strength bolts were utilized to connect the bottom end of specimens to the reaction frame and achieve a fixed end condition. To prevent global out-of-plane movement of the specimens, a lateral support frame was also provided, adjacent to the specimens. The horizontal actuator measured both the applied lateral displacements and lateral forces of a specimen. Furthermore, two linear variable displacement transducer (LVDT) was attached to the top and bottom of the specimens to measure the lateral displacements (Figure 5b). The top connection of the actuator to the specimens, shown in Figure (5c), was fabricated to establish the loading end in the form of pinned connection, to simulate the inflection point of the prototype column.

7. Testing Procedure

Each specimen was installed on rigid frame by high strength bolts and vertical and horizontal loading actuators were connected to the top beam of the reaction frame (Figure 5b). For the testing, the axial compression load was initially applied
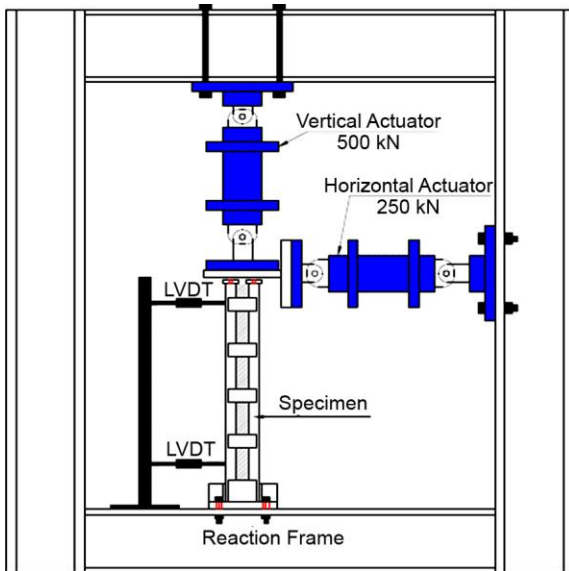
(a) Schematic Set-Up

(b) A Specimen Installatin

(c) Top Pinned Connection

Figure 5. Test set up.

to reach its predetermined magnitude. After that, the cyclic displacement protocol, proposed in ATC-24 [38], was applied horizontally to the specimens. In the loading protocol, shown in Figure (6), the first five drift amplitudes consisted of three-cycles and the other cycles had two-cycles. The yielding displacement of each specimen, lateral displacement corresponding the first yielding in section that is shown by Δ_y in Figure (6), was estimated by a finite element analysis. To achieve yielding point of specimens, Δ_y, the finite element based software ABAQUS was used.
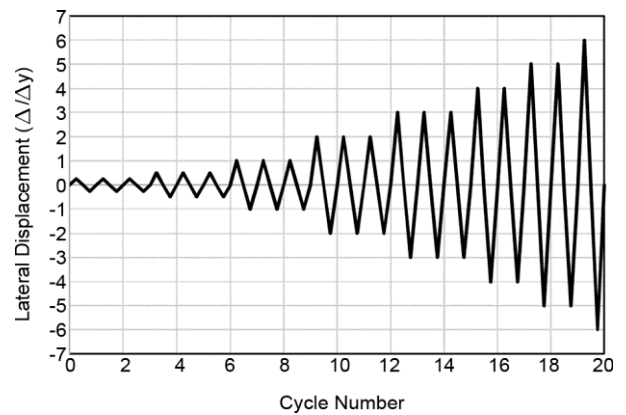

Figure 6. Lateral displacement protocol of specimens.

The behavior of steel was simulated by bi-linear curve that has elastic zone with modulus of elasticity (E_s) of 216 GPa and isotropic hardening zone with yield strength of f_y and tangent modulus of 0.01Es.

For concrete, damage plasticity model with isotropic damage was used for cyclic condition. The concrete elastic modulus, E_c, was determined as $4730\sqrt{f'_c}$ according to ACI318-11 [39] (f'_c is the cylindrical compressive stress, mentioned in Table 3), and Poisson's ratio was set as 0.20.

All components were modeled using an eight-node brick element (C3D8R) in the ABAQUS element library [40]. Steel components were connected to each other by tie interaction and contact element with friction was used to concrete-steel internal interface modeling.

As shown in Figure (7), CFBCs were fixed to the rigid floor by four high-strength bolts at the bottom and pinned at the top.

In the analyses, similar to the experiment, a constant axial compression was initially applied at the top of members and then the cyclic horizontal displacement in the X direction was applied.

In the analytical phase, various material definition, contact, interaction elements and boundary conditions have been considered to achieve the best simulation accuracy. However, to achieve confident results, the models should be verified by the experimental results.

The cyclic response of similar specimens, H35P1 (hollow) and F35P1 (filled) gained from the FE analysis were compared to results of the experimental phase in Figure (8) and Figure (9) respectively. As seen, in FE models, buckling modes have a true shape and were occurred at the same location of the experimental specimens. Moreover, the difference between the cyclic curve in FE models and experimental specimens were negligible.
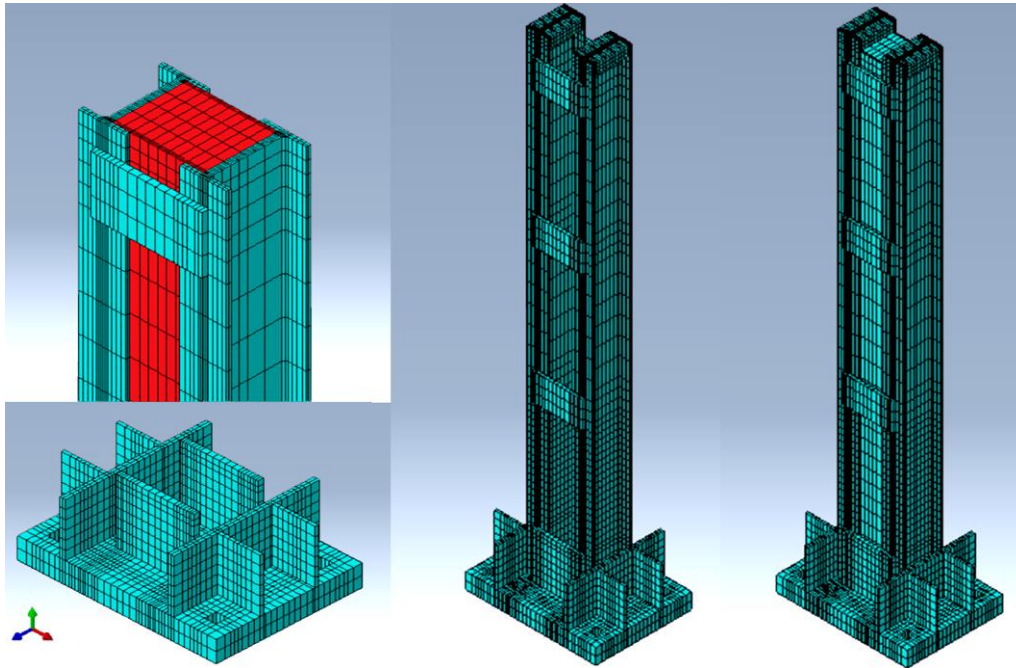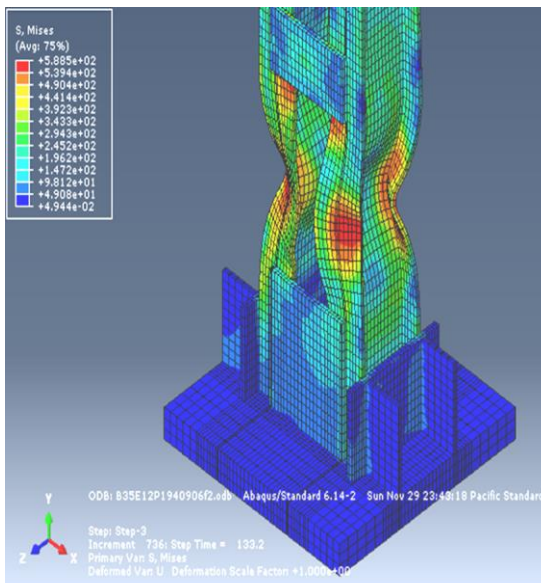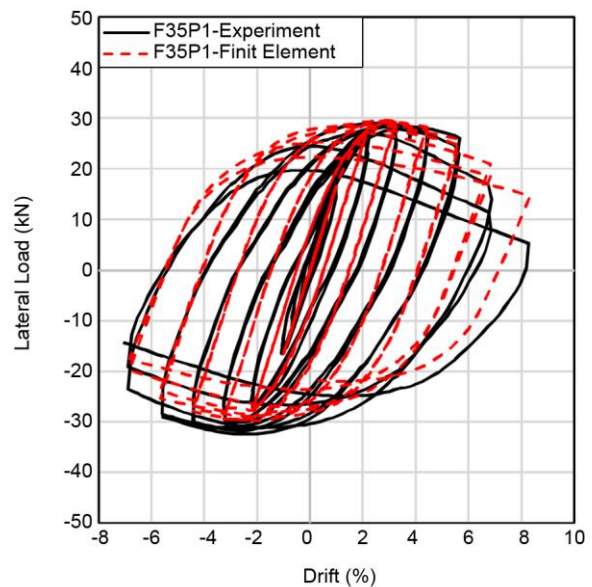

Figure 7. Finite element models assemblage.
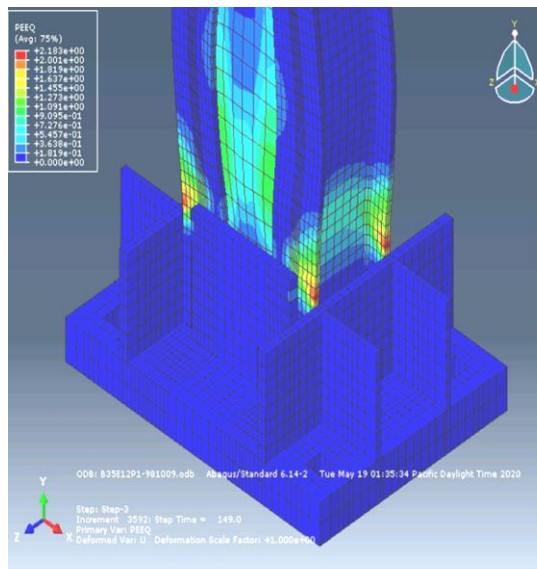

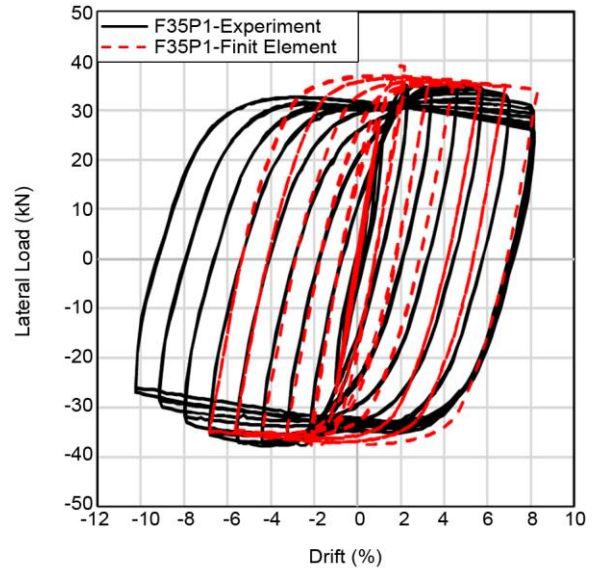(a) Buckling and Failure Mode

(b) Lateral Force-Lateral Displacement Loops

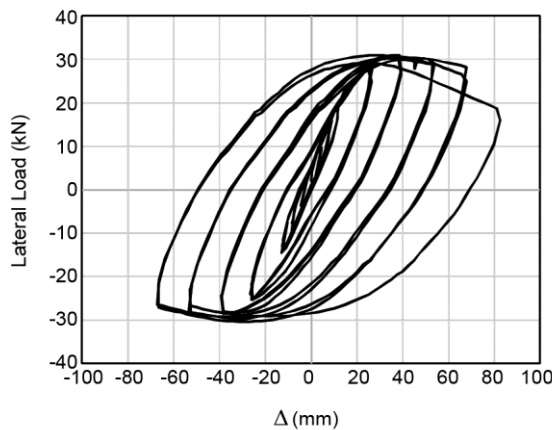**Figure 8.** Analytical cyclic curve and failure mode of H35P1.
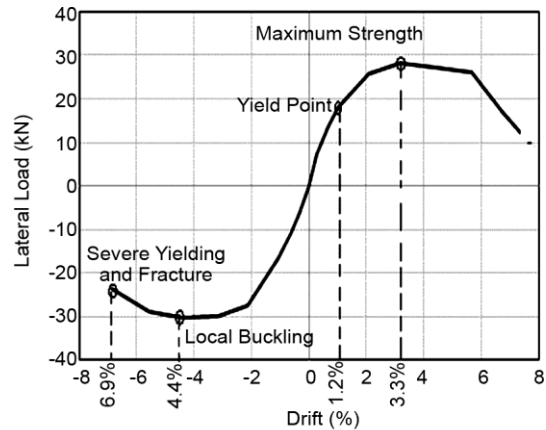
(a) Buckling and Failure Mode

(b) Lateral Force-Lateral Displacement Loops

Figure 9. Analytical cyclic curve and failure mode of F35P1.

(a) Lateral Force-Lateral Displacement Loops

(b) Envelope Curve with Substantial Events

Figure 10. Force - Displacement cyclic curve for H35P1.

8.1. Hollow Battened Specimen H35P1

As mentioned before, Specimen H35P1 was hollow with 350 mm battens spacing and considered as the reference sample. Lateral drift was defined as the ratio of lateral displacement to specimen height.

As seen in Figure (10), the cyclic curve remained elastic until 14.1 mm lateral displacement (1.2% lateral drift). Then, local buckling and yielding occurred in the flanges of steel sections at 4.4% lateral drift, and consequently, the slope of the load-deformation curve was decreased. Failure modes of the specimen, H35P1, for some drifts are shown in Figure (11). Pictures of the front and side views of

the specimen buckling are shown in Figure (12).

8.2. Filled Battened Specimen F35P1

Hysteresis behavior of filled battened specimen F35P1 is depicted in Figure (13). The hysteresis loops are not symmetric due to the actuator limitations: the horizontal actuator in one direction could not retract more than 100 mm, but in the reverse direction it did not have any limit. Hence in specimen F35P1, when lateral cyclic displacement attained to 100 mm, in the subsequent cycle, lateral displacement in one direction was kept constant but in the reverse direction, it was increased according to loading protocol shown in Figure (6).
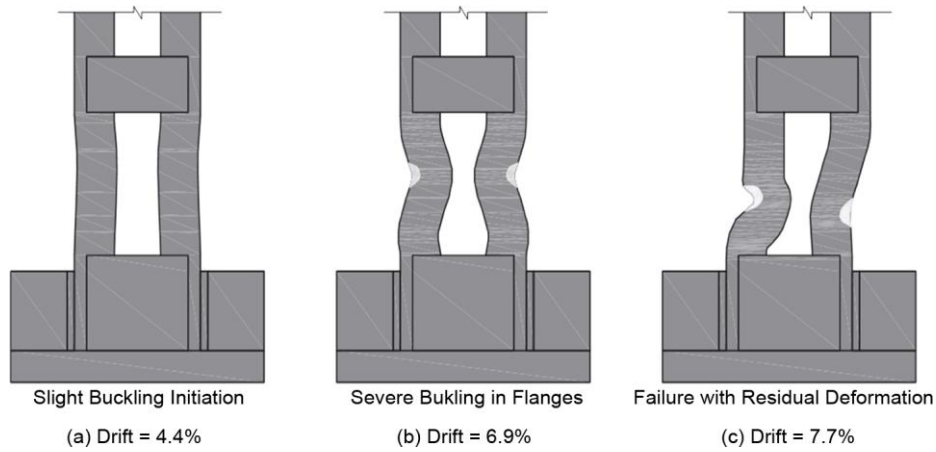
Slight Buckling Initiation   Severe Bukling in Flanges   Failure with Residual Deformation

(a) Drift = 4.4%   (b) Drift = 6.9%   (c) Drift = 7.7%

Figure 11. Deformed shape and failure mode of H35P1.

(a) Front View   (b) Side View
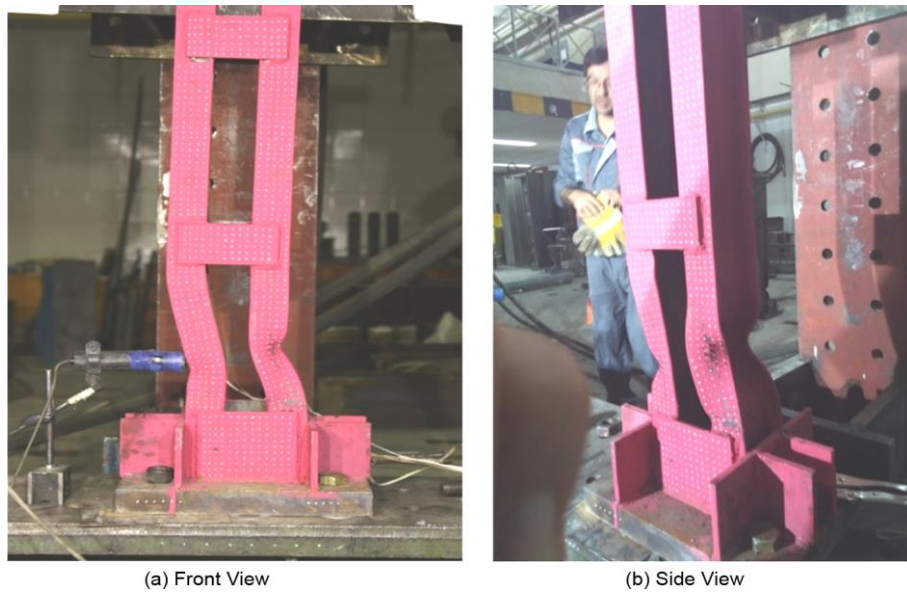
Figure 12. Deformed shape and failure mode of H35P1.

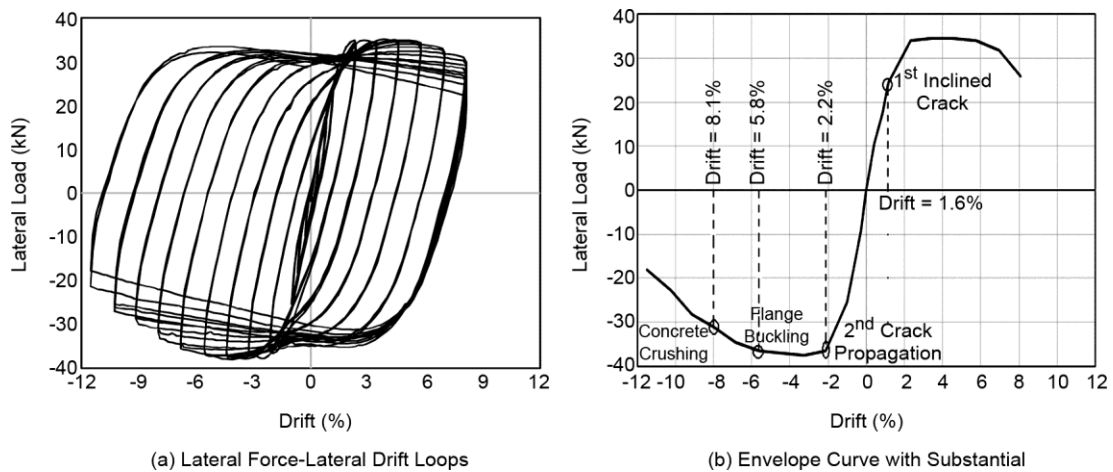(a) Lateral Force-Lateral Drift Loops   (b) Envelope Curve with Substantial

Figure 13. Force - Displacement cyclic curve for F35P1.

During the testing, the response of this specimen was linear up to lateral drift of 1.6%. The maximum lateral strength, 38.7 kN, was achieved at the lateral drift of 3.6% and remained constant in the subsequent four cycles. Then local buckling in flanges at the bottom of chords was

observed symmetrically outward at 3.8% lateral drift. The inclined cracks were opened and concrete crushing occurred. After that, severe buckling and yielding were seen. Finally, although the specimen was not severely damaged, the test was terminated because of actuator limitation, at the drift of 11.6% with the residual strength of 21.5 kN. Failure modes and concrete cracks of the specimen are shown in Figure (14) for different drift ratios. Pictures of front and side views of the specimen at the end of the testing are also shown in Figure (15).

8.3. Effect of In-Filled Concrete

In previous sections, cyclic behavior of hollow and similar filled specimens, H35P1 and F35P1, were studied. Their cyclic and envelope curves are compared in Figure (16).

Other filled specimens tested here were quite similar, in dimensions, material properties, boundary condition and loading mechanism, to hollow specimens tested by Hosseini Hashemi and Jafari [5].

Therefore, the behavior of tested filled specimens was compared with similar hollow ones tested by Hossieni Hashemi and Jafari [5] (Figures 17 to 19).

When filled with concrete, about fifty percent growth in ultimate lateral strength was seen and ductility increased about 25 to 40 percent.
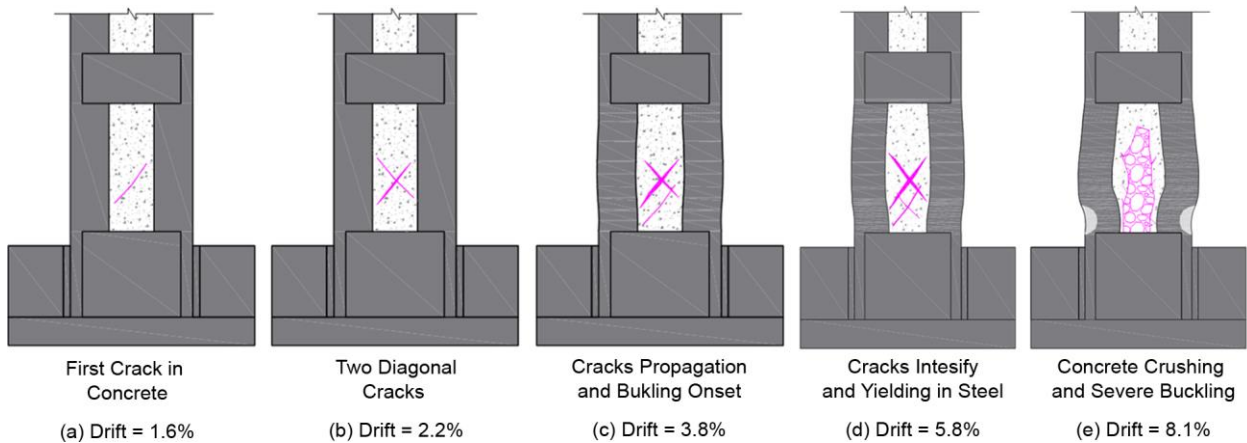

First Crack in Concrete	Two Diagonal Cracks	Cracks Propagation and Bukling Onset	Cracks Intesify and Yielding in Steel	Concrete Crushing and Severe Buckling
(a) Drift = 1.6%	(b) Drift = 2.2%	(c) Drift = 3.8%	(d) Drift = 5.8%	(e) Drift = 8.1%

Figure 14. Empirical performance of filled specimen F35P1.

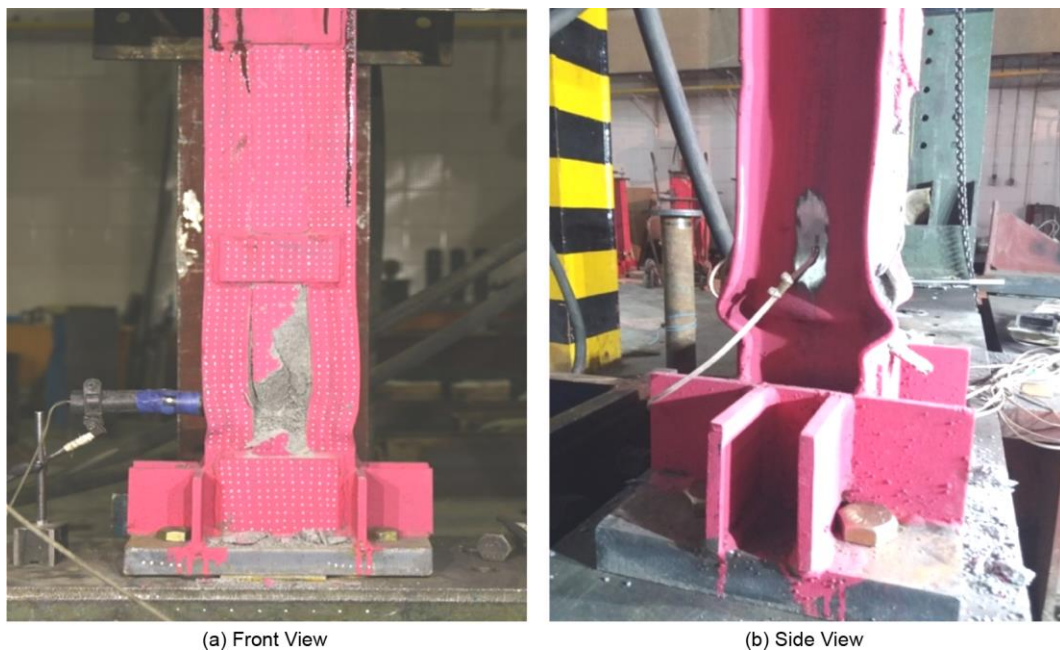(a) Front View   (b) Side View

Figure 15. Deformed shape of F35P1 at the end of test.

Furthermore, after ultimate strength, point (Q_m, Δ_m) in Figure (20), the filled specimens have flat post-yield response while hollow specimens experienced sudden descending response and it was important,

especially in ductile members. Local buckling in the hollow specimen was found more severe and started in a smaller drift amplitude range, in comparison with the similar filled ones.
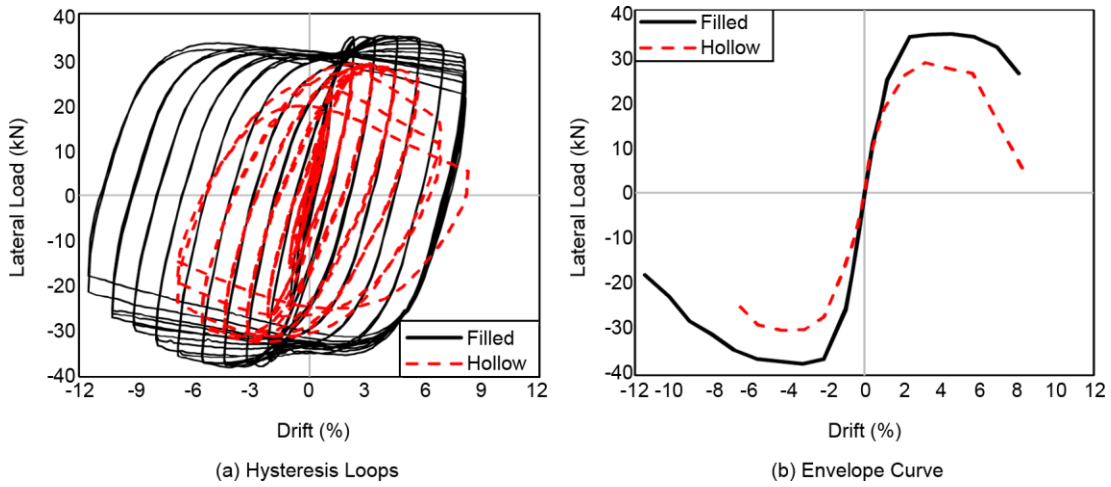

(a) Hysteresis Loops

(b) Envelope Curve

Figure 16. Hysteresis curves of hollow (B35P1) and similar filled specimen (F35P1).

(a) Hysteresis Loops

(b) Envelope Curve
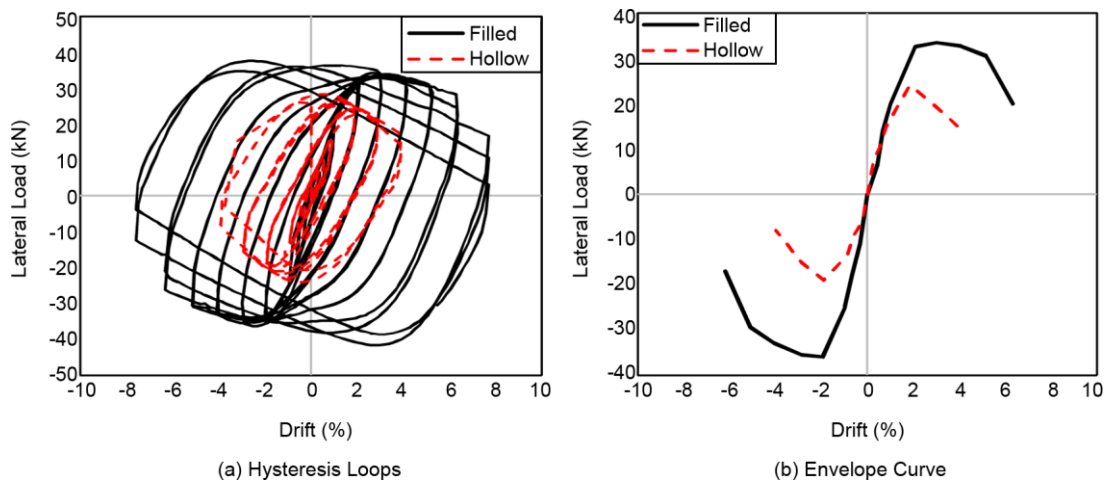
Figure 17. Hysteresis curves of hollow B35E12P2 [5] and similar filled specimen (F35P2).

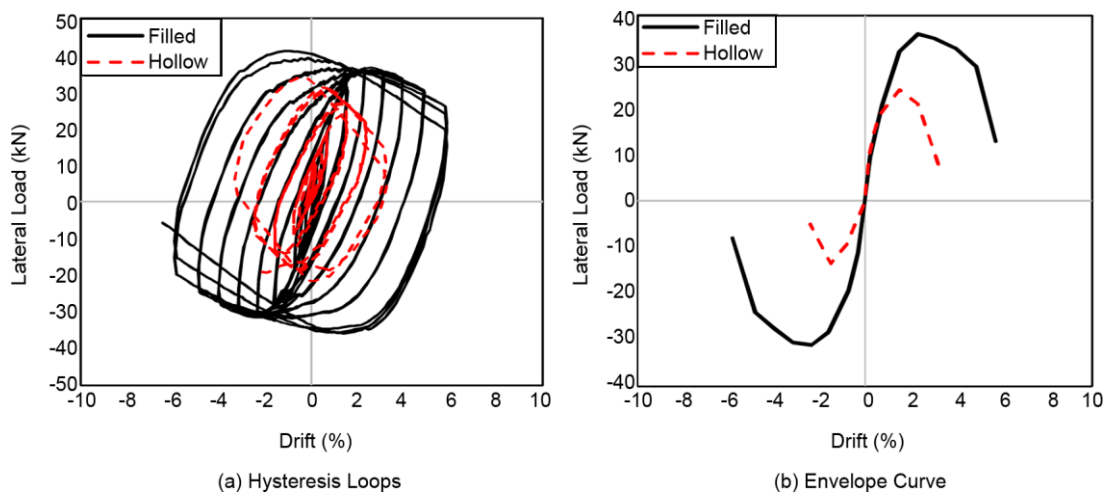(a) Hysteresis Loops

(b) Envelope Curve

Figure 18. Hysteresis curves of hollow (B35E12P3 [5]) and similar filled specimen (F35P3).
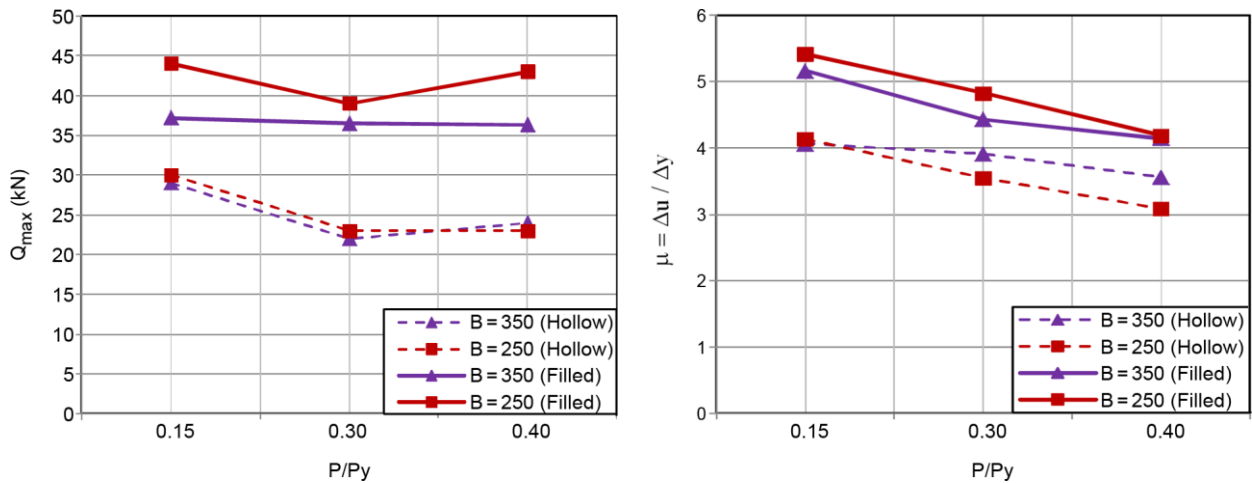
Figure 19. Ultimate strength and ductility of similar Filled and hollow specimens.

Table 4. Summary of test results.

Specimen	Specimen Properties						The Obtained Results					
	Steel Section	B (mm)	*h (mm)	Length (mm)	f'c (MPa)	Axial Load (P/Py)	Qe (kN)	Δe (mm)	Qm (kN)	Δm (mm)	Δu (mm)	μ= Δu / Δe
H35P1	2IPE100	350	120	1200	---	0.15	26	20	30.1	52.6	68	3.40
F35P1	2IPE100	350	120	1200	52	0.15	36	19	37.2	53	98	5.16
F35P2	2IPE100	350	120	1200	52	0.30	31	14	36.5	35	62	4.43
F35P3	2IPE100	350	120	1200	52	0.40	28	14	36.3	28	58	4.14
F25P1	2IPE100	250	120	1200	52	0.15	41	17	44	71	92	5.41
F25P2	2IPE100	250	120	1200	52	0.30	38	17	39	53	82	4.82
F25P3	2IPE100	250	120	1200	52	0.40	30	16	43	39	67	4.19

*h = distance between two I-section centroids.

8.4. Strength and Ductility in CFBCs

Strength and ductility were the most important parameters in structures in seismic zones. The specimens' properties and the resultant data are summarized in Table (4): the drift and strength of the yielding point are shown as Δ_e and Q_e, respectively. These quantities for the maximum strength are as Δ_m and Q_m and for the ultimate case are Δ_u and Q_u, which are all shown in Figure (20). Ductility, ultimate lateral strength and dissipated energy have an inverse correlation with the axial load level. The specimens' ductility are considered here as the ratio of Δ_u / Δ_e and will be calculated more accurately in the next part of this paper.

To show the influence of the axial load level, backbone curves of the filled specimens are compared in Figure (21). The specimens are also compared regarding their maximum strength and dissipated energy in Figure (22). The results show
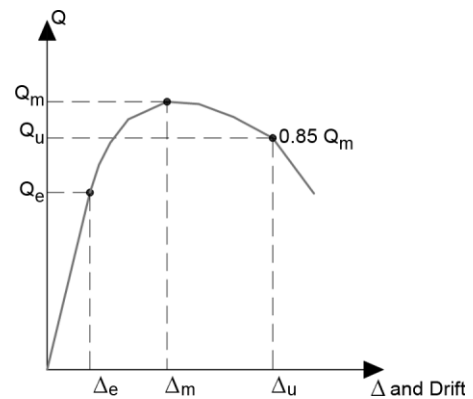

Figure 20. Yield and ultimate point on envelope curve.

that the axial load has an inverse effect not only on the specimen's ductility but also on the maximum strength and dissipated energy.

8.5. Ductility of the CFBCs

The backbone curves of the specimens are applied for ductility definition. The specimen's backbone curves are determined based on their

hysteresis curves by the ASCE41-17 method [37], shown for F35P1 in Figure (23). Backbone curves of the filled and similar hollow specimens for those having batten spacing of 350 and 250 mm, for all considered axial compression levels are shown in Figure (24) and Figure (25); it can be

seen that approximately in all twin specimens, the filled column has greater ductility.

8.6. Acceptance Criteria

Based on ASCE41-17, the nonlinear behavior of deformation-controlled elements is considered
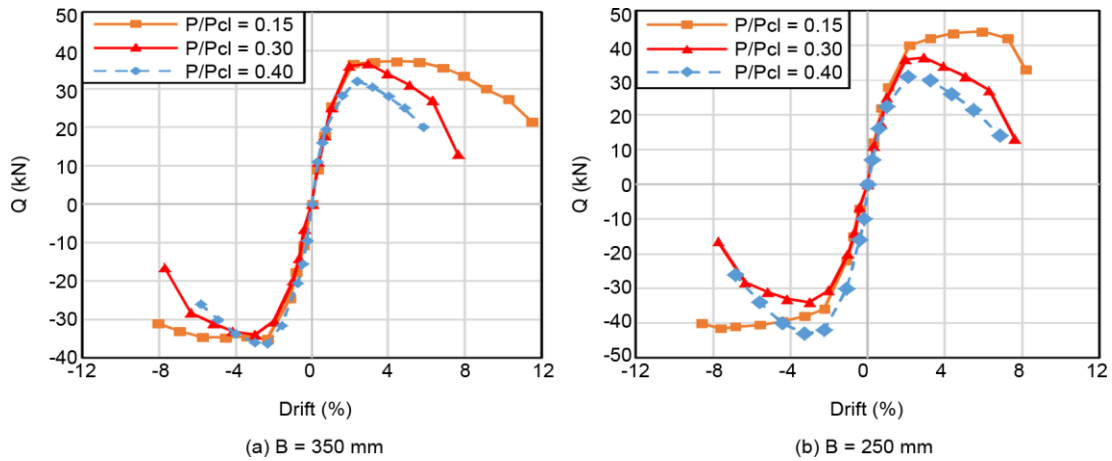

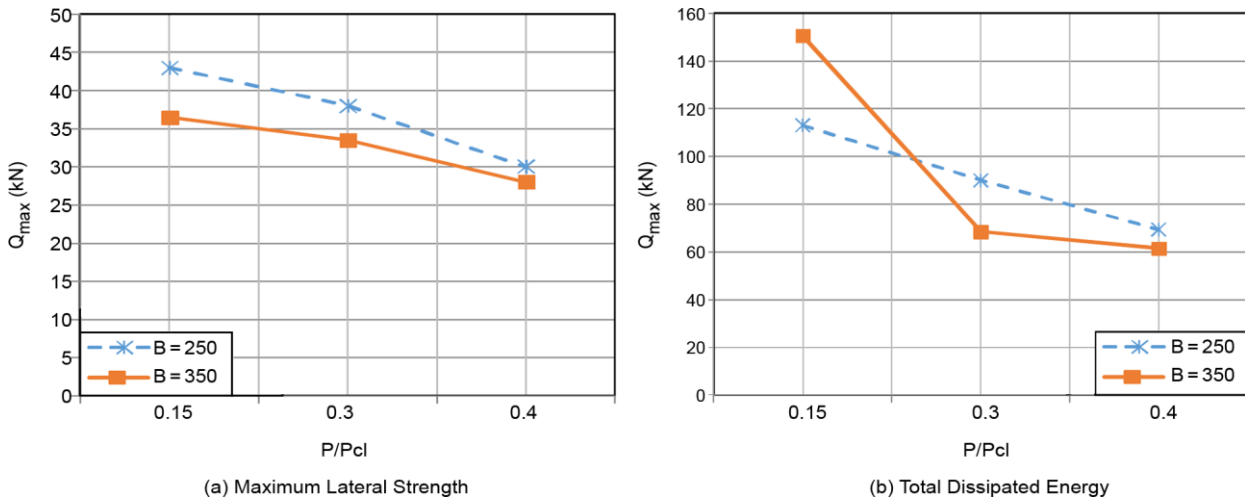**Figure 21.** Backbone curve of the filled specimens.

Figure 22. Effect of axial force and battens spacing in the filled columns.
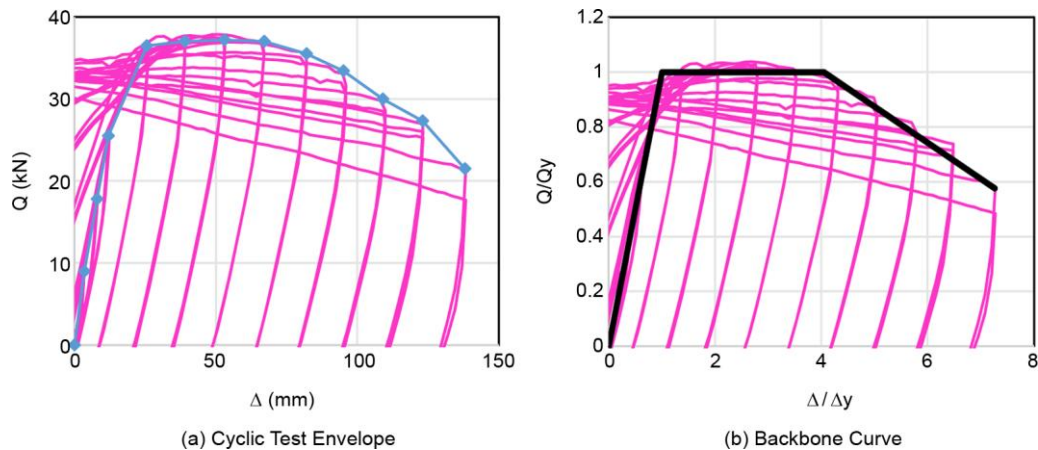

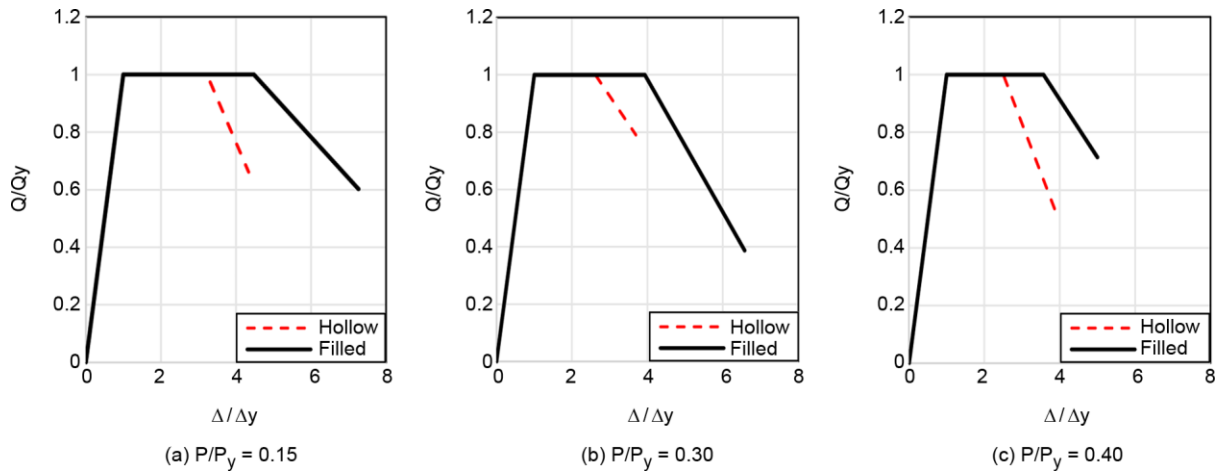**Figure 23.** Backbone curve for filled specimen (F35P1).

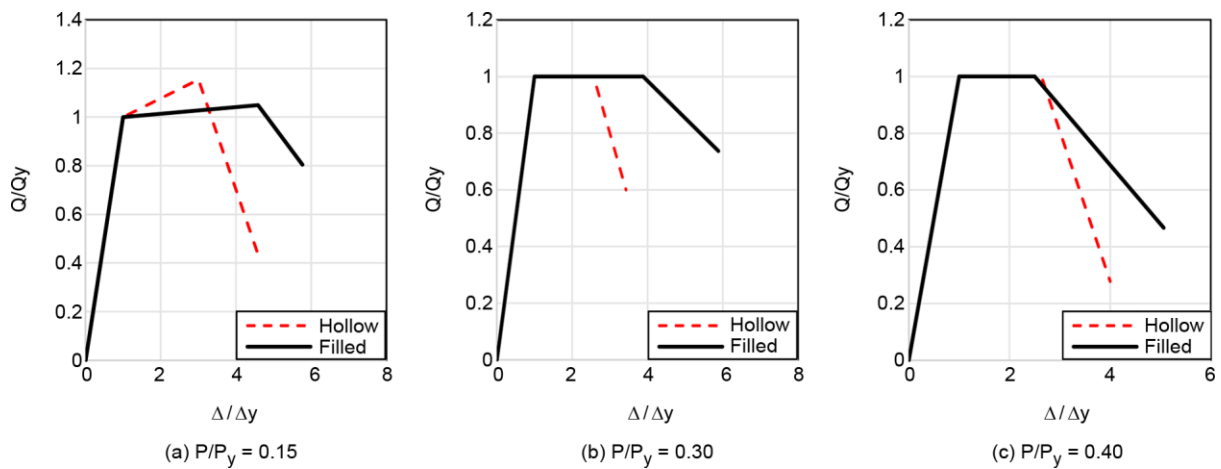**Figure 24.** Backbone curve for hollow [5] and similar filled specimen with B= 350 mm.

Figure 25. Backbone curve for hollow [5] and similar filled specimen with B = 250 mm.

Table 5. Values of the m-factor for tested specimens.

Dimension	Specification	m (LS)	m (CP)
B35P1	Hollow	1.91	2.33
F35P1	Filled with Concrete	2.52	3.36
B35E12P2 [7]	Hollow	1.47	1.96
F35P2	Filled with Concrete	2.21	2.95
B35E12P3[7]	Hollow	1.41	1.88
F35P3	Filled with Concrete	2.01	2.68
B25E12P1[7]	Hollow	1.69	2.25
F25P1	Filled with Concrete	2.58	3.24
B25E12P2[7]	Hollow	1.45	1.93
F25P2	Filled with Concrete	2.18	2.91
B25E12P3[7]	Hollow	1.48	1.98
F25P3	Filled with Concrete	1.41	1.88

by component capacity modification factor "m-factor". Based on ASCE 41-17, the m-factor for Life Safety (LS) and Collapse Prevention (CP) level are 0.56 (Δ_C/Δ_B) and 0.75 (Δ_C/Δ_B), respectively. Δ_B and Δ_C are the displacements of the yielding point and the point corresponding to the strength downfall, respectively. M-factor of the concrete-filled battened specimens, as well as the corresponding reference specimens, summarized in Table (5).

9. Conclusion

In this experimental research, concrete-filled and hollow battened columns were tested and compared under cyclic lateral loading. Each specimen has been tested under constant axial and cyclic lateral loading. To investigate the influence of the axial load, different axial load levels, including $0.15\,P_y$, $0.3\,P_y$ and $0.4\,P_y$ were considered for the specimens (P_y is the axial yield strength of the hollow column). The obtained results are as follows:

− The failure mode in hollow and filled battened columns was local buckling of the I-sections (both in flanges and web), but the intensity of local buckling in filled columns is much less and local buckling mode of bottom chords is different.

− When battened columns are filled with concrete, the dissipated energy increases up to six times in comparison with hollow ones. Also, the slope of the post yielding curve decreased but residual strength was substantial.

− In the filled specimens, the results show that the distance between battens has a poor effect on cyclic behavior of battened steel columns but the magnitude of axial compression load has a significant effect.

− Axial load has a detracting influence on the behavior of specimens, increasing the axial load from $0.15\,P_y$ to $0.4\,P_y$, decreases the ductility up to 30% and the lateral load up to 41%. The component capacity modification factor "m-factor" of a filled specimen is up to 47% higher than that of the similar hollow one regarding that filling with concrete raises both the ductility and the strength. This method can be used to strengthen fragile hollow battened columns.

Acknowledgement

References

1. Ministry of Housing and Urban Development, Tehran (2013) *Iranian National Building Code, Part 10: Steel Structures*, 4th Edition.

2. AISC-LRFD (2005) *Load and Resistance Factor Design Specifications for Structural Steel Buildings*.

3. Kleiser, M. and Uang, C.M. (1999) Steel latticed members under cyclic axial and flexural actions. *Journal of Structural Engineering (ASCE)*, **125**(4), 393-400.

4. Sahoo, D. and Rai, D.C. (2004) Batten built-up beam-columns under cyclic loads. *13th World Conference on Earthquake Engineering*, Vancouver, B.C., Canada, paper no. 67.

5. Hosseini Hashemi, B. and Jafari, M. (2012) Experimental evaluation of cyclic behavior of batten columns. *Journal of Constructional Steel Research*, **78**, 88-96.

6. Hosseini Hashemi, B. and Poursamad Bonab, A. (2013) Experimental investigation of the behavior of laced columns under constant axial load and cyclic lateral load. *Engineering Structures*, **57**, 536-543.

7. Hosseini Hashemi, B. and Poursamad Bonab, A. (2012) Analytical investigation of cyclic behavior of laced built-up columns. *Journal of Constructional Steel Research*, **73**, 128-138.

8. Hosseini Hashemi, B. and Jafari, M. (2004) Performance of batten columns in steel buildings during the Bam earthquake of 26 December 2003. *Journal of Seismology and Earthquake Engineering (JSEE)*, **5**(4), 101-109.

9. Hosseini Hashemi, B. and Kiany, B.K. (2019) Performance of steel structures and associated lessons to be learned from November 12, 2017, Sarpol-e Zahab-Ezgeleh Earthquake (MW 7.3). *Journal of Seismology and Earthquake Engineering*, **20**(3), 33-46.

10. Tomii, M. and Yoshimaro, K. (1977) Experimental studies on concrete filled steel tubular columns under concentric loading. *International Colloquium on Stability of Structures under Static and Dynamic Loads*,

Washington, DC., 718-741.

11. Okamato, T. and Maeno, T. (1988) Experimental Study on Rectangular steel tube columns infilled with Ultra high strength concrete. *Annual Meeting of AIJ, Proceedings Chiba*, 1359.

12. Yoshika, Y. (1992) State of art of composite steel tube and concrete structures in Japan. *US-Japan Workshop on Composite and Hybrid Structures, Proceedings*, Berkeley, California, 119-130.

13. Nagashima, T. and Sugano, S. (1989) An experimental study on behavior of concrete-filled steel tubular columns under cyclic loading axial load. *Abstract, Annual Meeting of A.I.J.*, 1601-1602.

14. Liang, Q.Q. (2009) Performance-based analysis of concrete-filled steel tubular beam-columns, Part I: Theory and algorithms. *Journal of Constructional Steel Research*, **65**(2), 363-372.

15. Patel, V.I., Liang, Q.Q., and Hadi, M.N.S. (2014) Numerical analysis of high-strength concrete-filled steel tubular slender beam-columns under cyclic loading. *Journal of Constructional Steel Research*, **92**, 183-194.

16. Ahmed, M., Liang, Q.Q., Patel, V.I., and Hadi, M.N.S. (2018) Nonlinear analysis of rectangular concrete-filled double steel tubular short columns incorporating local buckling. *Engineering Structures*, **175**, 13-26.

17. Han, L.-H., Zhao, X.-L., and Tao, Z. (2001) Tests and mechanics model for concrete-filled SHS stub columns, columns and beam-columns. *Steel and Composite Structures*, **1**, 51-74.

18. Lam, D. and Williams, C.A. (2004) Experimental study on concrete filled square hollow sections. Steel and Composite Structures, **4**(2), 95-112.

19. Ghannam, S., Abdeljavad, Y., and Hunait, Y. (2004) Failure of lightweight aggregate concrete-filled steel tubular columns. *Steel and Composite Structures*, **4**(1), 1-8.

20. Campione, G. and Scibilia, N. (2002) Beam-column behavior of concrete filled steel tubes. *Steel and Composite Structures*, **2**(4), 259-276.

21. Ishizawa, T., Nakano, T., and Iura, M. (2006) Experimental study on partially concrete-filled steel tubular columns. *Steel and Composite Structures*, **6**(1), 55-69.

22. Zhao, X., Grzebieta, R., and Elchalakani, M. (2002) Tests of concrete-filled double skin CHS composite stub columns. *Steel and Composite Structures,* **2**(2), 129-146.

23. Wu, B., Lin, L., Zhao, J., and Shen, C. (2020) Compressive behaviour of thin-walled square tubular columns filled with high-strength steel section and precast compound concrete segments. *Thin-Walled Structures*, **151**:106710.

24. Li, W., Chen, B., Han, L., and Lam, D. (2020) Experimental study on the performance of steel-concrete interfaces in circular concrete-filled double skin steel tube. *Thin-Walled Structures*, **149**(9):106660.

25. Ye, Y., Li, W., and Guo, Z. (2020) Performance of concrete-filled stainless steel tubes subjected to tension: experimental investigation. *Thin-Walled Structures*, **148**:106602.

26. Usami, T., Susantha, K., and Hanbin G. (2001) Confinement evaluation of concrete-filled box-shaped steel columns. *Steel and Composite Structures,* **1**(3), 313-328.

27. Usami, T., Ge, H. (1992) Strength of concrete filled thin walled steel box columns: experiment. *Journal of Structural Engineering*, **118**(11), 3036-3054.

28. Usami, T. and Ge, H. (1994) Ductility of concrete filled steel box columns under cyclic loading. *Journal of Structural Engineering*, **120**(7), 2021-2040.

29. Mamaghani, I.H.P., Usami, T., and Mizuno, E. (1996) Cyclic elastoplastic large displacement behavior of steel compression members.

Journal of Structural Engineering, **42A**, 135-145.

30. Hunaiti, Y., Wakabayashi, M., and Kiyoshi, M. (1992) Experimental evaluation of the effect of bond on the maximum capacity of composite columns. *Journal of Constructional Steel Research*, **22**, 39-55.

31. Taylor, R., Shakir-Khalil, H., and Yee, M. (1983) Some tests on a new type of composite column. *Proceedings of the Institution of Civil Engineers*, **75**(2), 283-296, Part 2.

32. Elzbieta, S., Zoltowski, W., and Siennicki, M. (2010) Research on load capacity of concrete filled columns with battened steel sections. *Journal of Civil Engineering and Management*, **16**(3), 313-319.

33. Zoltowski, W., Szmigiera, E., and Siennicki, M. (2006a) The behavior of steel-concrete composite columns with battened steel sections. *XIth International Conference on Metal Structures, Progress in Steel, Composite and Aluminium Structure*, Rzeszów, Poland, 212-213.

34. Zoltowski, W., Szmigiera, E., and Siennicki, M. (2006b) The influence of concrete filling steel columns with two battened chords on their behavior. *8th International Conference on Steel, Space & Composite Structures, Kuala Lumpur, Malaysia*, 417-423.

35. Mehrabani, R. and Shanmugam, N.E. (2014) Finite element analysis of the behavior and ultimate strength of battened columns encased in concrete. *The IES Journal Part A: Civil & Structural Engineering*, **7**(4), 263-280.

36. Venugopal, R., Shanmugam, N.E., and Richard Liew, J. (2003) Built-up columns encased in concrete. *Advances in Structures Proceedings of International Conference ASSCCA*, **2**, 759-764.

37. ASCE (2017) *ASCE/SEI, 41-17, Seismic Evaluation and Retrofit of Existing Buildings*. ASCE Standard, American Society of Civil Engineers Reston, Virginia.

38. Applied Technology Council (1992) *ATC-24: Guidelines for Cyclic Seismic Testing of Components of Steel Structures*. Redwood City, California.

39. American Concrete Institute (2011*) Building Code Requirements for Structural Concrete and Commentary*. ACI 318-11, Detroit.

40. Hibbitt, Karlson and Sorensen, Inc. (2005) *ABAQUS Version 6.5: Theory Manual, Users' Manual, Verification Manual and Example Problems Manual*.